Articles

Discovery of Small-Molecule Inhibitors of Bcl-2 through Structure-Based Computer Screening

Istvan J. Enyedy,[†,‡,§] Yan Ling,[†,‡] Kassoum Nacro,[†] York Tomita,[†] Xihan Wu,[†,⊥] Yeyu Cao,[†,⊥] Ribo Guo,[†] Bihua Li,[†] Xiaofeng Zhu,[†] Ying Huang,[†] Ya-Qiu Long,[∥] Peter P. Roller,[∥] Dajun Yang,*[,†] and Shaomeng Wang*[,†,⊥]

Structural Biology and Cancer Drug Discovery Program, Lombardi Cancer Center and Department of Oncology, Georgetown University Medical Center, 3970 Reservoir Road, Washington, D.C. 20007, and Laboratory of Medicinal Chemistry, National Cancer Institute, FCRDC, Building 376, Room 207, Fredrick, Maryland 21702

Received January 10, 2001

Bcl-2 belongs to a growing family of proteins which regulates programmed cell death (apoptosis). Overexpression of Bcl-2 has been observed in 70% of breast cancer, 30−60% of prostate cancer, 80% of B-cell lymphomas, 90% of colorectal adenocarcinomas, and many other forms of cancer. Thereby, Bcl-2 is an attractive new anti-cancer target. Herein, we describe the discovery of novel classes of small-molecule inhibitors targeted at the BH3 binding pocket in Bcl-2. The three-dimensional (3D) structure of Bcl-2 has been modeled on the basis of a high-resolution NMR solution structure of Bcl-X_L, which shares a high sequence homology with Bcl-2. A structure-based computer screening approach has been employed to search the National Cancer Institute 3D database of 206 876 organic compounds to identify potential Bcl-2 small-molecule inhibitors that bind to the BH3 binding site of Bcl-2. These potential Bcl-2 small-molecule inhibitors were first tested in an in vitro binding assay for their potency in inhibition of the binding of a Bak BH3 peptide to Bcl-2. Thirty-five potential inhibitors were tested in this binding assay, and seven of them were found to have a binding affinity (IC_{50} value) from 1.6 to 14.0 μM. The anti-proliferative activity of these seven active compounds has been tested using a human myeloid leukemia cell line, HL-60, which expresses the highest level of Bcl-2 protein among all the cancer cell lines examined. Compound **6** was the most potent compound and had an IC_{50} value of 4 μM in inhibition of cell growth using the 3-(4,5-dimethylthiazol-2-yl)-2,5-diphenyltetrazolium bromide assay. Five other compounds had moderate activity in inhibition of cell growth. Compound **6** was further evaluated for its ability to induce apoptosis in cancer cells. It was found that **6** induces apoptosis in cancer cells with high Bcl-2 expression and its potency correlates with the Bcl-2 expression level in cancer cells. Furthermore, using NMR methods, we conclusively demonstrated that **6** binds to the BH3 binding site in Bcl-X_L. Our results showed that small-molecule inhibitors of Bcl-2 such as **6** modulate the biological function of Bcl-2, and induce apoptosis in cancer cells with high Bcl-2 expression, while they have little effect on cancer cells with low or undetectable levels of Bcl-2 expression. Therefore, compound **6** can be used as a valuable pharmacological tool to elucidate the function of Bcl-2 and also serves as a novel lead compound for further design and optimization. Our results suggest that the structure-based computer screening strategy employed in the study is effective for identifying novel, structurally diverse, nonpeptide small-molecule inhibitors that target the BH3 binding site of Bcl-2.

Introduction

Apoptosis, or programmed cell death, is important for normal development, host defense, and suppression of oncogenesis, and faulty regulation of apoptosis has been implicated in cancer and many other human diseases.[1−3] The Bcl-2 family of proteins now includes both anti-apoptotic molecules such as Bcl-2 and Bcl-X_L and pro-apoptotic molecules such as Bax, Bak, Bid, and Bad.[1−3] These molecules play crucial roles in regulating apoptosis. A simplified Bcl-2-mediated apoptosis pathway is provided in Figure 1. The ability of Bcl-2 and Bcl-X_L to form heterodimmers with a number of pro-apoptotic proteins such as Bak, Bad, and Bax is believed to play a crucial role for the anti-apoptotic function of Bcl-2 and Bcl-X_L, although the precise molecular mechanism of action of Bcl-2 remains far from completely understood.

As an anti-apoptotic member of this family, Bcl-2 contributes to cancer cell progression by preventing normal cell turnover caused by physiological cell death mechanisms. Overexpression of Bcl-2 has been observed in 70% of breast cancer, 30−60% of prostate cancer, 80% of B-cell lymphomas, 90% of colorectal adenocarcinomas, and many other forms of cancer.[4] The expression levels

* Address correspondence and requests for reprints to Shaomeng Wang [phone (734) 615-0362; fax (734) 647-9647; e-mail shaomeng@umich.edu] or Dajun Yang [phone (202) 687-0265; fax (202) 687-7505; e-mail yangd@georgetown.edu].

[†] Georgetown University Medical Center.

[‡] These authors contributed equally to this work.

[§] Present address: Bayer Pharmaceutical Division, 400 Morgan Lane, West Haven, CT 06516.

[∥] National Cancer Institute.

[⊥] Present address: 3316 CCGC, University of Michigan Cancer Center, 1500 E. Medical Center, Ann Arbor, MI 48109.

10.1021/jm010016f CCC: $20.00
Published on Web 11/01/2001

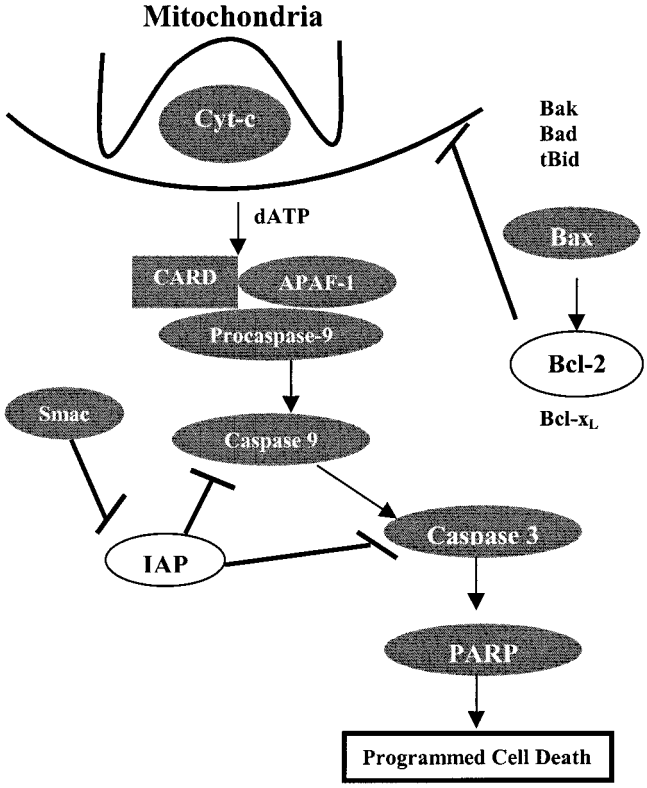

Figure 1. A simplified Bcl-2-mediated signaling pathway of programmed cell death.

of Bcl-2 proteins also correlate with resistance to a wide spectrum of chemotherapeutic drugs and γ-radiation therapy.[5−7] Biological approaches targeted at Bcl-2 using anti-sense oligonucleotides or single-chain antibodies have been shown to enhance tumor cell chemosensitivity.[8−13] Recently, cell-permeable Bcl-2 binding peptides containing a fatty acid have been shown to induce apoptosis in vitro and have in vivo activity in suppressing human myeloid leukemia growth in severe combined immunodeficient mice.[14] Therefore, Bcl-2 represents an attractive target for the development of a novel therapy for the treatment of many forms of cancer.

Certain possible limitations are associated with large-molecule and peptide approaches, including poor oral availability, poor in vivo stability, and/or high cost. We are therefore interested in the discovery and design of nonpeptide, small-molecule inhibitors that target Bcl-2 and modulate its anti-apoptotic function. A potent, cell-permeable Bcl-2 small-molecule inhibitor can serve as a valuable pharmacological tool to further elucidate the biological function of Bcl-2 in vitro and in vivo. Furthermore, such an inhibitor may have great therapeutic potential as a novel therapy for the treatment of many forms of cancer, either alone or in combination with conventional chemotherapy or radiation therapy.

It has been traditionally difficult to discover small-molecule inhibitors to block protein−protein interactions. Thus, despite the successful development of several screening assays, discoveries of small-molecule inhibitors of Bcl-2 remained elusive for several years. However, more recently, three independent groups reported their discovery of small-molecule inhibitors of Bcl-2/Bcl-X_L. The very first report on the discovery of a small-molecule inhibitor of Bcl-2 was contributed by

Chart 1. Small-Molecule Inhibitors of Bcl-2 (or Bcl-X_L) Reported to Date

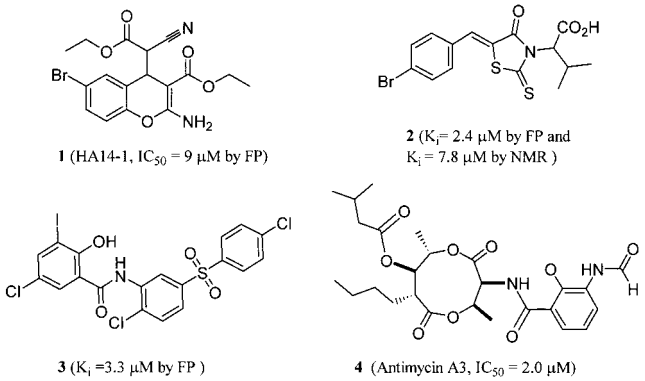

Huang's laboratory.[15] Using a computerized structure-based database screening strategy, Dr. Huang and his colleagues screened the Available Chemical Directory of more than 200 000 small organic compounds and discovered one class of small organic molecules (called HA14-1) that bind to the BH3 binding site in Bcl-2 (**1**, Chart 1). HA14-1 effectively induced apoptosis in human acute myeloid leukemia (HL-60) cells overexpressing Bcl-2 protein. Although the potency of this small organic inhibitor is only moderate (IC_{50} = 9 μM in binding assay), this study clearly showed that it is possible to design a nonpeptide, small-molecule inhibitor of Bcl-2.

Very recently, two independent papers reported the discovery of three new classes of small-molecule inhibitors of Bcl-2 or Bcl-X_L.[16,17] Using a high-throughput screening assay based upon fluorescene polarization, Dr. Yuan and colleagues screened a library of 16 320 chemicals and identified two different classes of small-molecule inhibitors of Bcl-X_L. The most potent representative compounds are shown in Chart 1 (compounds **2** and **3**).[16] Dr. Hockenbery and colleagues identified antimycin A (compound **4** in Chart 1), an antibiotic, as a small-molecule inhibitor of Bcl-2/Bcl-X_L with an IC_{50} value of 2 μM.[17] Taken together, these three studies showed that a small organic molecule inhibitor that binds to the BH3 domain in Bcl-2/Bcl-X_L can inhibit their anti-apoptotic function, which in turn induces apoptosis in cells with Bcl-2/Bcl-X_L overexpression. These exciting discoveries strongly indicated that it is possible to design small-molecule inhibitors that block the interactions between Bcl-2/Bcl-X_L and pro-apoptotic proteins (peptides) such as Bak, Bad, and Bax, and inhibit the biological function of Bcl-2/Bcl-X_L.

In recent years, the structure-based approach has become very powerful for the discovery of novel lead compounds and for lead optimization. Herein, we report the discovery of several classes of novel small-molecule inhibitors of Bcl-2 through structure-based computer screening of the National Cancer Institute three-dimensional (3D) database and the characterization in biochemical and cellular assays. Furthermore, we have investigated the interactions of a promising small-molecule inhibitor (**6**) with Bcl-X_L through NMR methods and conclusively confirmed that **6** binds to the BH3 binding site in Bcl-X_L.

Results and Discussion

Homology Modeling of the Bcl-2 3D Structure. Structure-based database searching requires an ac-

```
Bcl2      5    NREIVMKYIHYKLSQRGYEWDAGDVGAAPPGAAPAPGIFSSQP  47
               NRE+V+ ++ YKLSQ+GY W            AP     +
Bcl-XL    5    NRELVVDFLSYKLSQKGYSWSQFSDVEENRTEAPEG---TESE  44

Bcl2      88   VVHLTLRQAGDDFSRRYRRDFAEMSRQLHLTPFTARGRFATVV  130
               +V   LR AGD+F  RYRR F +++ QLH+TP TA   F  VV
Bcl-XL    85   AVKQALREAGDEFELRYRRAFSDLTSQLHITPGTAYQSFEQVV  127

Bcl2      131  EELFRDGVNWGRIVAFFEFGGVMCVESVNREMSPLVDNIALWM  173
                ELFRDGVNWGRIVAFF FGG+ CVESV++EM  LV  IA+WM
Bcl-XL    128  NELFRDGVNWGRIVAFFSFGGALCVESVDKEMQVLVSRIAAWM  170

Bcl2      174  TEYLNRHLHTWIQDNGGWDAFVELYG   199
                 YLN HL  WIQ+NGGWD+FVELYG
Bcl-XL    171  ATYLNDHLEPWIQENGGWDTFVELYG   196
```

Figure 2. Sequence alignment between Bcl-2 and Bcl-X_L.

curate 3D structure of Bcl-2. The experimental 3D structures of Bcl-2 are now available.[18] However, when we started the project, the experimental Bcl-2 structure was not determined. Fortunately, high-resolution experimental 3D structures of Bcl-X_L[19−21] alone and in complex with a Bak BH3 (Bcl-2 homology domain 3) peptide[21] have been determined. Bcl-2 and Bcl-X_L share a high degree of homology in their amino acid sequences (45% identity and 56% similarity). It has been demonstrated that when there is a sequence identity of more than 30% between the target protein (Bcl-2) and the template protein (Bcl-X_L), current computational homology modeling methods, such as MODELLER,[24] can provide an accurate 3D structure for the target protein.[25] Therefore, computational homology modeling was employed to model the 3D structure of Bcl-2 (the target protein) on the basis of the experimental 3D structural coordinates of Bcl-X_L (the template protein) in this study.

The sequence alignment obtained using the BLAST program[22,23] between Bcl-2 and Bcl-X_L is provided in Figure 2, which was used in our homology modeling. Since the Bak BH3 peptide binds to both Bcl-2 and Bcl-X_L with good affinities,[14,15] the 3D structure of Bcl-2 in complex with the Bak BH3 peptide was modeled on the basis of the experimental NMR structure of Bcl-X_L in complex with the Bak BH3 peptide.[21] Using the MODELLER program,[24−26] 10 different models were generated. It was found that these 10 models were very similar, with a root-mean-square deviation (RMSD) within 1 Å for all the non-hydrogen atoms of residues that form the BH3 binding site. To further refine the side chain conformations, the modeled 3D complex structure was extensively simulated through molecular dynamics (MD) simulation in explicit water for 3 ns. Comparison of our modeled Bcl-2 structure with the recently published experimental high-resolution Bcl-2 NMR structure[18] showed that they are essentially the same with respect to both the overall fold and binding site conformation. The RMSD is 1.0 Å for all the non-hydrogen atoms of residues that form the BH3 binding site between the NMR structure[18] and our modeled structure. Thus, computational homology modeling provided us with an accurate 3D structure of Bcl-2 for our structure-based 3D database search. The refined structure of Bcl-2 in complex with the Bak BH3 peptide is depicted in Figure 3.

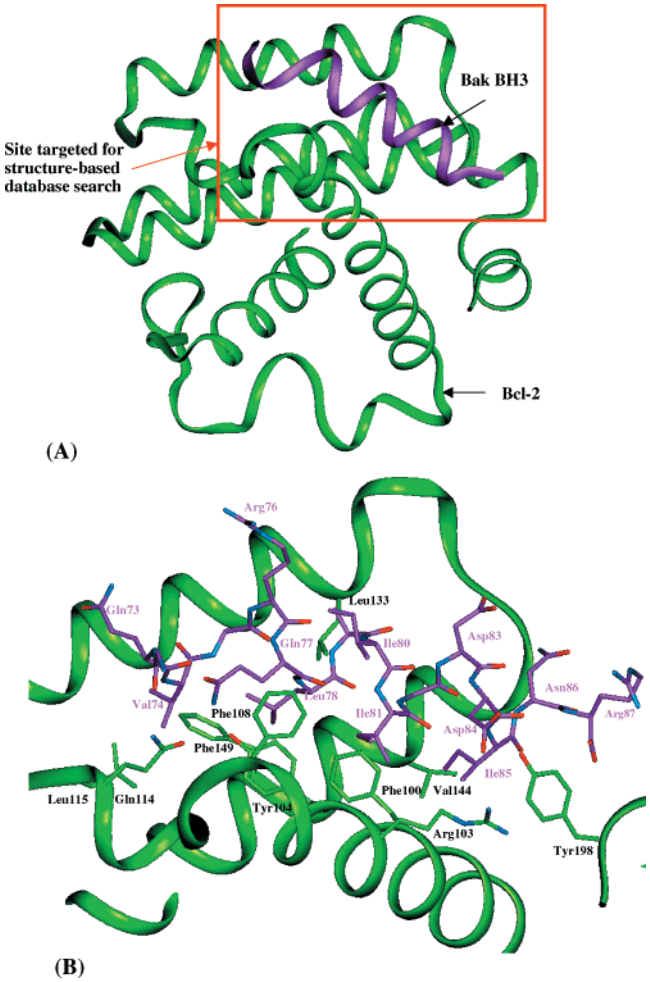

Figure 3. Modeled 3D structure of Bcl-2 in complex with the Bak BH3 domain based upon the experimental structure of Bcl-X_L in complex with the Bak BH3 peptide (PDB code 1BXL). (A) Ribbon representation of the overall Bcl-2 structure in complex with the Bak BH3 peptide. (B). Detailed representation of the binding site. The carbon atoms in the Bak BH3 peptide are shown in magenta, the carbon atoms in the Bcl-2 protein in green, the oxygen atoms in red, and the nitrogen atoms in blue.

Defining the "Binding" Site for Structure-Based Computer Screening. The experimental structure of Bcl-X_L in complex with the Bak BH3 peptide[21] as well as our modeled structure of Bcl-2 in complex with the

Table 1. Chemical Structures and Binding Affinities of Active Compounds

	Structure	Binding IC_{50} (μM)		Structure	Binding IC_{50} (μM)
5	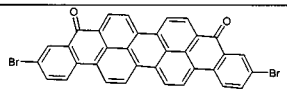	7.7 ± 4.5	**9**	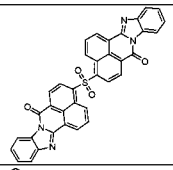	14.0 ± 2.8
6	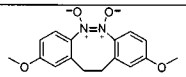	10.4 ± 0.3	**10**	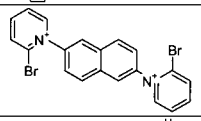	11.7 ± 2.4
7	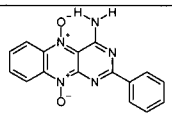	1.6 ± 0.1	**11**	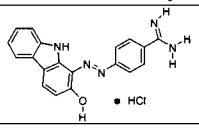	5.8 ± 2.2
8	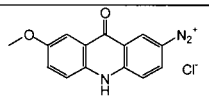	10.4 ± 1.2			

Bak BH3 peptide provided us with a structural basis for their interactions between these proteins.

The Bak BH3 peptide binds to the largely hydrophobic binding pocket formed by the BH1, BH2, and BH3 domains in Bcl-2 as well as in Bcl-X_L. This binding pocket in Bcl-2 appears to be essential for its anti-apoptotic function since mutations at this site abolish its function.[28,29] Furthermore, synthetic, cell-permeable peptides binding to this pocket in Bcl-2 induce apoptosis in vitro and have in vivo activity in suppressing human myeloid leukemia growth.[14,30] Nonpeptide small-molecule Bcl-2 inhibitors **1**−**4** that bind to this pocket have been shown to compete with the Bak BH3 peptide in binding to Bcl-2 in vitro and induce apoptosis.[15] Taken together, these data provide strong evidence that the hydrophobic binding pocket formed by the BH1, BH2, and BH3 domains of Bcl-2 is an attractive site for the design of nonpeptide, small-molecule inhibitors of Bcl-2 for modulating its function. Accordingly, all residues that are within 8 Å from the Bak peptide in the Bak-Bcl-2 complex were selected and used to define the binding site for identification of potential Bcl-2 inhibitors in our subsequent structure-based computer screening.

Structure-Based Computer Screening of the National Cancer Institute 3D Database To Identify Potential Bcl-2 Small Molecules. Since 1955, the National Cancer Institute (NCI) at the National Institutes of Health has conducted extensive testing of materials for possible activity against different forms of cancer. Most of the substances tested have been pure organic compounds. The program examined an extraordinarily eclectic assembly of organic structures. Currently, more than 465 000 compounds have been tested.[31] Of these compounds, about half (206 876 compounds) are classified as "open" compounds, whose structures and biological data can be accessed by the public.[31] Because samples of compounds were needed for testing, it was necessary to develop a large acquisition effort and a repository, both of which are still functioning today. Continual scanning of the chemistry literature allows identification of compounds that are novel and of interest to the program, and the authors are approached for a sample, typically under 100 mg. Currently, the NCI repository has physical samples of about 60% of the registered compounds. Recently, analysis of several large chemical databases showed that the NCI database has by far the highest number of compounds that are unique to it.[32] Approximately 200 000 of the NCI structures are not found in any of the other six analyzed databases.[32] Therefore, the NCI open database provides a large number of unique synthetic compounds and natural products and is an excellent resource for drug lead discovery.

Using the modeled 3D structure of Bcl-2, we searched the NCI 3D database of 206 876 small molecules using the program DOCK.[33,34] In the database search, conformational flexibility of the small molecules was taken into account. The small molecules were ranked according to their scores as calculated using the energy scoring function in the DOCK program. The top 500 candidate small molecules with the best scores were considered as potential Bcl-2 inhibitors. Only nonpeptide molecules were selected for testing. In the first batch of biological testing, samples of 80 compounds were requested from the NCI and 35 compounds were available for testing.

Results of the Binding Assay. We have used a sensitive and quantitative in vitro fluorescence polarization (FP) based binding assay.[15] The basic principle behind this assay is competition: a fluorescent peptide tracer (Flu-Bak-BH3) and a nonfluorescent small-molecule inhibitor compete for binding to the target protein (Bcl-2). In a reaction mixture containing no small-molecule inhibitor, the fluorescent tracer Flu-Bak-BH3 is bound to the target protein Bcl-2 and the emission signal is polarized; however, in a reaction mixture containing a small-molecule inhibitor, the tracer is displaced by the small-molecule inhibitor from the target protein and the emission signal becomes depolarized. The resulting change in the FP signal is directly related to the inhibitory activity of the small-molecule inhibitor. Using this method, a binding affinity of 0.3 μM (IC_{50}) was obtained for Bak-BH3 peptide binding to the Bcl-2, which is consistent with the value reported in the literature.[15]

The binding affinity of the 35 candidate small molecules was tested initially at a dose of 100 μM in this

Table 2. Chemical Structures of Inactive Compounds

	Structure		Structure		Structure
12	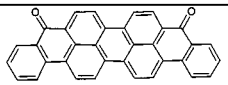	**22**	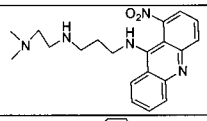	**31**	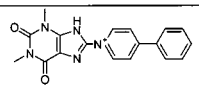
13	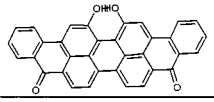	**23**	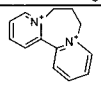	**32**	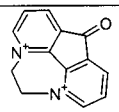
14	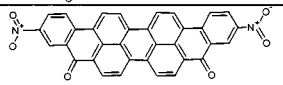	**24**	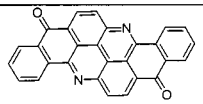	**33**	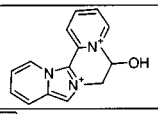
15	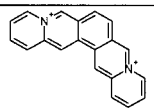	**25**	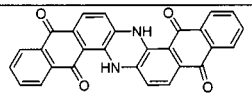	**34**	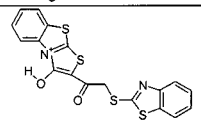
16	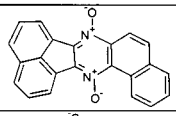	**26**	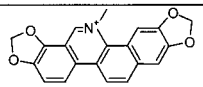	**35**	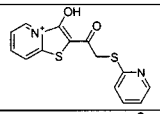
17	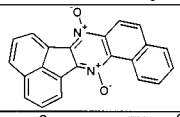	**27**	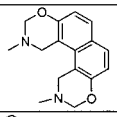	**36**	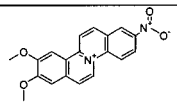
18	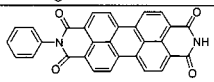	**28**	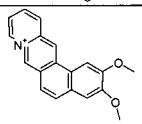	**37**	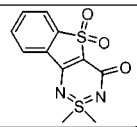
19	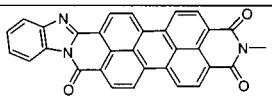	**29**	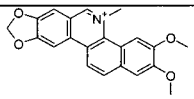	**38**	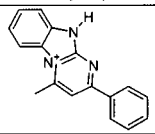
20	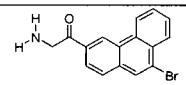	**30**	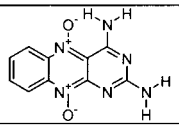	**39**	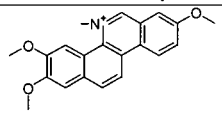
21	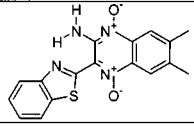				

binding assay, of which 7 compounds showed inhibitory activity of more than 50% at the initial 100 μM dose level and were classified as active. The other 28 compounds had less than 50% inhibition at the 100 μM dose level and were classified as inactive. Further dose-dependent binding experiments were carried out for these seven active compounds to determine their IC_{50} values. All seven active compounds displayed a dose-dependent inhibition of Bak peptide binding to Bcl-2. The chemical structures and IC_{50} values of these seven active compounds are provided in Table 1. The chemical structures of the 28 inactive compounds are provided in Table 2.

As can be seen from Table 1, all of these seven active compounds have an IC_{50} value better than 15 μM. Compound **7** is the most potent compound in the binding assay, with an IC_{50} value of 1.6 μM. The other six compounds have an IC_{50} value from 5.8 to 14.0 μM. It is of note that all of these seven active compounds belong to different chemical classes and their structures are also different from those of the previously reported Bcl-2 inhibitors **1**−**4**.

A previous study showed that screening of 16 320 compounds using a high-throughput screening approach has led to the discovery of two chemical classes of small-molecule inhibitors of Bcl-2/Bcl-X_L.[16] In our study, testing of 35 compounds selected from structure-based 3D database screening allowed the discovery of 7 classes of small-molecule inhibitors of Bcl-2. Our results thus suggested that the structure-based computer screening strategy employed in this study is effective in identifying novel small-molecule inhibitors of Bcl-2.

Inhibition of Cell Viability and Growth in Cancer Cells with High Bcl-2 Expression. Binding experiments showed that these seven active compounds are capable of competing with the Bak BH3 peptide in binding to Bcl-2 in vitro. Since we are interested in identifying cell-permeable Bcl-2 small-molecule inhibitors, we have tested the inhibitory activity of these

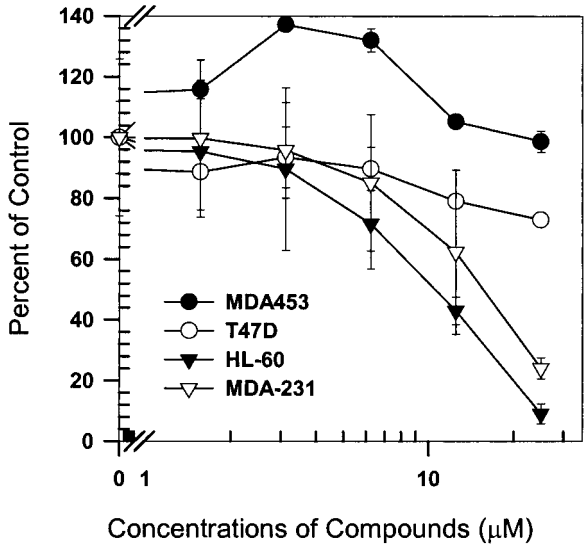

Figure 4. Effects of compound **6** on cell viability in cancer cell lines with different levels of Bcl-2 protein expression.

seven active compounds on cell viability and proliferation using two different assays. First, the trypan blue exclusion method was used to determine the effect of an inhibitor on cell viability in which cells were treated with the inhibitor for 24 h. Second, the 3-(4,5-dimethylthiazol-2-yl)-2,5-diphenyltetrazolium bromide (MTT) assay was used to determine the activity of an inhibitor on cell proliferation where cells were treated for 4 days. It is important to keep in mind that an active compound in the binding assay could fail to show any cellular activity simply because of its poor cellular permeability. We first tested these seven active compounds using the HL-60 cell line. HL-60 is a human myeloid leukemia cell line and expresses the highest level of Bcl-2 protein among all the cancer cell lines examined in our laboratories (Figure 5).

Using the trypan blue exclusion assay, these seven compounds were screened for their activity in inhibition of cell viability. All seven compounds except for compound **10** had an IC_{50} value better than 50 μM. Compound **6** is the most potent compound in the cellular assay, with an IC_{50} value of 10 μM, as shown in Figure 4. We have further tested compound **6** for its ability to inhibit cell growth. In the MTT assay where cells were treated for 4 days, **6** showed a potent inhibition in cell growth with an IC_{50} value of 4 μM. Because of its potent cellular activity, **6** was used in subsequent biological experiments.

Chemical Structure Verification of the Active Compounds. One problem we and other investigators have encountered when using the NCI database is that samples of some compounds from the NCI repository are not pure, or may have decomposed over the years, or in rare cases the structures are simply wrong. Care was taken to verify the structures of the small-molecule inhibitors of Bcl-2 shown in Table 1.

First, we have performed mass spectral analyses on the samples of these seven compounds. The results are shown in Table 3. As can be seen, five compounds were found to have an observed mass in agreement with the calculated mass based upon the chemical structures. However, two compounds, **9** and **10**, were found to have an observed mass not in agreement with the calculated mass, suggesting that the chemical structures for these two compounds as recorded in the NCI database are incorrect.

Next, we obtained ^{1}H NMR spectra for these five active compounds whose structures are consistent with the mass spectral data. We were unable to obtain the ^{1}H NMR spectrum for compound **5** because it is in-

Table 3. Results of Mass Spectral Analysis of the Active Compounds in Table 1

	Structure	Calculated Mass (M)	Observed Mass		Structure	Calculated Mass (M)	Observed Mass
5	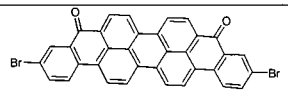	611.94	613.2 $(M+H)^+$	**9**	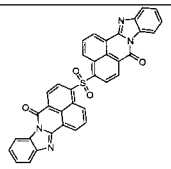	602.10	1241.8 $(M)^+$ or 352.3 $(M)^-$
6	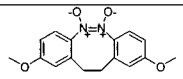	300.11	300.9 $(M+H)^+$	**10**	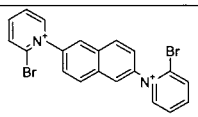	597.79	538 $(M)^-$
7	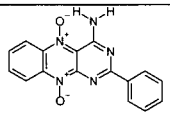	305.05	305.4 $(M)^-$	**11**	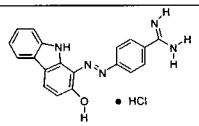	365.10 329.10 (-HCl)	330.1 $(M+H)^+$
8	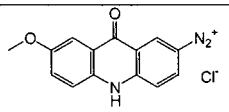	258.04 (with Cl^-) 222.06 (no Cl^-)	222.1 $(M)^+$				

Scheme 1. Synthetic Scheme of Compound **6**

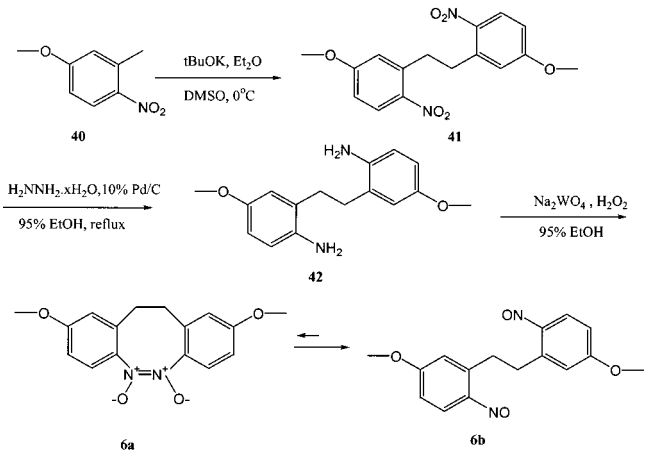

soluble in either DMSO or chloroform. The ^{1}H NMR spectra for compounds **6**−**8** and **11** are consistent with their chemical structures.

Compound **6** potently inhibits the cell viability (Figure 4) and growth, thus representing a novel class of cell-permeable small-molecule inhibitors of Bcl-2 and a promising lead compound for further design and chemical modifications. Accordingly, we have synthesized this compound to confirm conclusively its chemical structure.

Chemical Synthesis of Compound 6. The general synthesis procedure of compound **6** is illustrated in Scheme 1, according to a method developed by Bown and Greene.[35] Briefly, commercially available 3-methyl-4-nitroanisole (**40**) was dimerized to give compound **41** in 64% yield by oxidation with tBuOK and ether in DMSO. The diamino derivative **42** was obtained in excellent yield by reducing **41** in the presence of hydrazine hydrate and a catalytic amount of palladium. Oxidation of **42** with hydrogen peroxide and sodium tungstate dihydrate in ethanol gave compound **6** in 61% yield. It was previously shown that compound **6** was in tautomeric equilibrium (1:3.68 at 295.70 K in chloroform).[35] On the basis of our own NMR data, we estimated that the ratio between **6a** and **6b** is 1:3.69−3.79 in chloroform or 1:2.52 in DMSO at room temperature, respectively. Mass spectral and ^{1}H NMR analyses of the synthesized sample of compound **6** showed that it is identical to that acquired from the NCI repository. We further confirmed that the two samples of compound **6** have the same affinity for binding to Bcl-2 in the FP-based binding assay and have the same cellular activity in the HL-60 cell line. Accordingly, our subsequent studies on this compound were performed using the sample synthesized in our laboratory.

Specificity of 6 in Inhibition of Cell Viability. We showed that Bcl-2 inhibitor **6** blocks the binding of the Bak BH3 peptide to Bcl-2 in vitro and potently inhibits cell viability and growth in the HL-60 cell line with high Bcl-2 expression. Next we further tested the specificity of Bcl-2 inhibitors such as **6** in cancer cell lines with different levels of Bcl-2 expression to investigate whether **6** can achieve specific inhibition of cell viability and whether its cellular activity is dependent upon the level of Bcl-2 protein in cancer cells.

For this purpose, we have first characterized Bcl-2 protein expression in human breast and other cancer cell lines, and the results are shown in Figure 5. Human

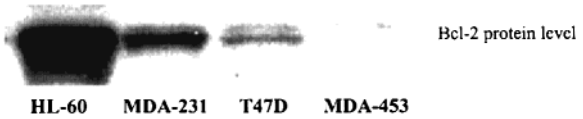

Figure 5. Level of Bcl-2 protein expression in cancer cell lines as detected by Western blotting. Human myeloid leukemia cell line HL-60 expresses the highest level of Bcl-2 protein among all the cell lines examined. MDA-231 (subclone 2LMP derived from our laboratory) expresses a high level of Bcl-2; T47D expresses a very low but detectable level of Bcl-2, whereas MDA-453 does not express detectable Bcl-2.

myeloid leukemia cell line HL-60 expresses the highest level of Bcl-2 protein among all the cell lines examined. MDA-231 (subclone 2LMP derived from our laboratory) expresses a high level of Bcl-2; T47D expresses a very low but detectable level of Bcl-2, whereas MDA-453 does not express detectable Bcl-2. Accordingly, we chose MDA-231 and HL-60 cell lines with high Bcl-2 expression as the positive cells and MDA-453 and T47D as the negative control cells to test the specificity of **6** in inhibition of cell viability using the trypan blue exclusion assay, as well as in our apoptosis experiments. The results are shown in Figure 4.

As can be seen, in HL-60 and MDA-231 cells, two cell lines with high Bcl-2 expression, **6** displays a dose-dependent inhibition of cell viability with IC_{50} values of 10 and 15 μM, respectively. In T47D cells, which have low but some level of Bcl-2 expression, **6** has a minimal activity at 25 μM. Furthermore, in MDA-453 cells, which have no detectable level of Bcl-2, **6** has no effect on cell viability at 25 μM. Therefore, the ability of **6** in inhibition of cell viability correlates with the Bcl-2 protein expression level in these cancer cells.

Induction of Apoptosis. One central hypothesis we wanted to test is that the binding pocket formed by the BH1, BH2, and BH3 domains in Bcl-2 is essential for its anti-apoptotic function, and binding of a small-molecule inhibitor such as **6** to this pocket may block the anti-apoptotic function of Bcl-2 and induce apoptosis in cells with Bcl-2 protein overexpression. To test this hypothesis, we evaluated the ability and very importantly the specificity of **6** in inducing apoptosis in cancer cells with a high or low level of Bcl-2 expression.

We used the Annexin-V flow cytometry assay to obtain a quantitative assessment on the ability of **6** in induction of apoptosis in HL-60 and MDA-231 cells. MDA-231 cells treated with 0 (untreated), 5, and 10 μM **6** for 24 h exhibited 0%, 13%, and 20.0% apoptotic cells, respectively, while HL-60 cells treated with 0, 5, 10, and 20 μM **6** for 24 h had 0%, 24%, 31%, and 67% apoptotic cells, respectively. Therefore, **6** induced apoptosis in a dose-dependent manner in MDA-231 and HL-60 cell lines with Bcl-2 protein overexpression.

Taken together, our results showed that **6** specifically induces apoptosis in a dose-dependent manner in cancer cells with high Blc-2 expression while it has little effect on cancer cells with low or little Bcl-2 expression. Our data suggested that overexpression of Bcl-2 may be necessary to maintain the transformed state in these cancer cells and that blocking the Bcl-2 anti-apoptotic function with a small-molecule inhibitor such as **6** will induce apoptosis in these cancer cells.

Confirmation of the Binding of 6 to Bcl-X_L by NMR. Using the FP-based assay, we showed that **6**

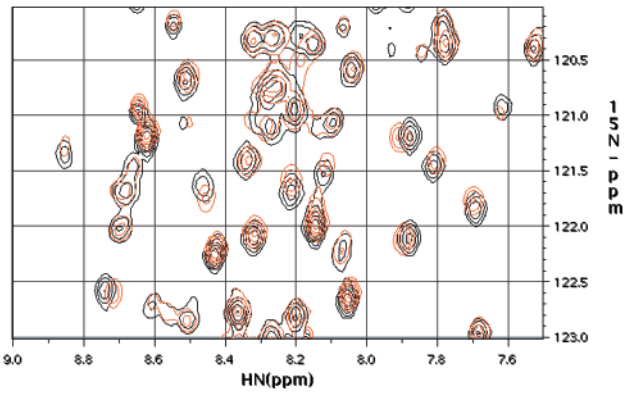

Figure 6. Superposition of ^{15}N HSQC spectra of ^{15}N-labeled Bcl-X_L protein in free form (black) and in complex with **6** (red).

binds to Bcl-2. However, the in vitro FP-based method simply shows that addition of a small-molecule inhibitor reduces the intensity of FP. The most straightforward interpretation is that the small-molecule inhibitor binds to Bcl-2 and displaces the binding of the fluorescence-labeled Bak BH3 peptide. However, it is also possible that addition of the small-molecule inhibitor simply causes the unfolding of the protein and thus reduces the binding of the fluorescence-labeled Bak BH3 peptide to the protein. To rule out the latter possibility, we have employed NMR methods to conclusively show that **6** indeed binds to the protein and does not unfold the protein.

Wild-type Bcl-2 behaves poorly in solution even if the putative hydrophobic transmembrane region is deleted and is thus not amenable to structure determination by either NMR spectroscopy or X-ray crystallography. Very recently, the problem of poor solubility of wild-type Bcl-2 was elegantly circumvented by using Bcl-2/Bcl-X_L chimeras in which part of the putative unstructured loop of Bcl-2 was replaced with a shortened loop from Bcl-X_L.[18] However, wild-type Bcl-X_L is soluble if the putative hydrophobic transmembrane region is deleted.[19,21] Bcl-2 and Bcl-X_L are closely related homologous proteins and have very similar 3D structures. We have recently determined the affinity of binding of **6** to Bcl-X_L using a FP binding assay for Bcl-X_L and showed that **6** binds to Bcl-X_L with an IC_{50} value of 7 μM, similar to that of binding to Bcl-2. Furthermore, Bcl-X_L and Bcl-2 are structurally very similar. Thus, it is highly likely **6** binds to Bcl-2 and Bcl-X_L in very similar binding modes. Since Bcl-X_L behaves much better in solution,[19,21] we chose to use Bcl-X_L for our NMR experiments.

We measured the hetereonuclear single-quantum correlation (HSQC) spectrum of ^{15}N-labeled Bcl-X_L without and with **6**. The HSQC spectrum is also called a fingerprint spectrum because of its sensitivity to structural changes. As can be seen from Figure 6, the binding of **6** caused the peak shifts of only several residues, strongly suggesting that **6** causes only local perturbation in the structure of Bcl-X_L but not overall folding of Bcl-X_L. Furthermore, most of the residues whose chemical shifts are affected by the binding of **6** were around the BH3 binding pocket of Bcl-X_L (Figure 7). Therefore, our NMR HSQC experiments conclusively showed that **6** binds to the BH3 binding site in Bcl-X_L and does not unfold the protein. We are currently undertaking efforts to determine the 3D structure of **6** in complex with Bcl-X_L, and the results will be reported in due course.

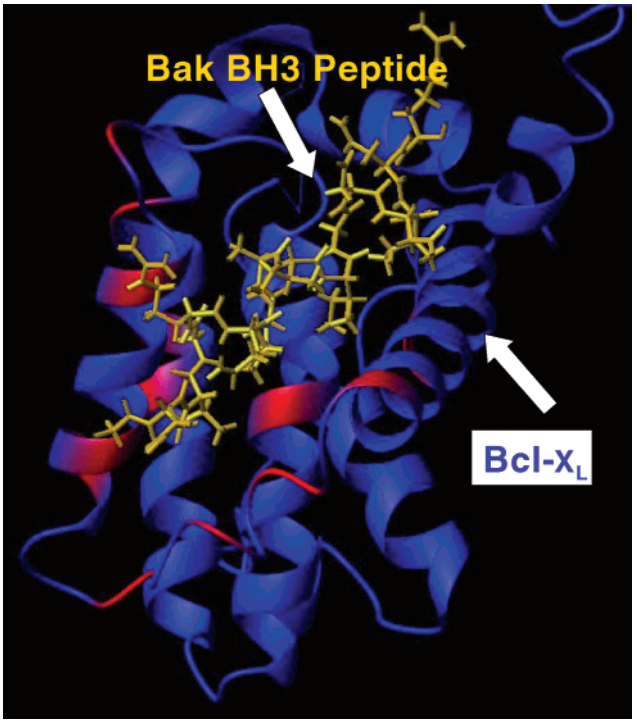

Figure 7. The residues in Bcl-X_L whose chemical shifts are affected by the binding of **6** are shown in red. The 3D structure of Bcl-X_L is shown in ribbon representation in blue, and the BH3 peptide is shown in licorice representation in yellow. The NMR experimental structure of Bcl-X_L in complex with the Bak BH3 peptide is used to depict the locations of these residues. This figure was prepared using the MOLMOL program.[38]

Summary

Through structure-based computer screening of the NCI 3D database and biological testing of a limited number of potential Bcl-2 inhibitors, we have identified seven classes of novel Bcl-2 inhibitors with IC_{50} values ranging from 1.6 to 14.0 μM in the FP-based binding experiments. To verify the chemical structures of these small-molecule inhibitors, we performed mass and ^{1}H NMR analyses on the chemical samples. The mass and ^{1}H NMR data for five small-molecule inhibitors are consistent with their chemical structures recorded in the NCI database. However, the mass data for two active compounds are inconsistent with their chemical structures recorded in the NCI database. Therefore, it is recommended that when the NCI database is used for drug discovery, the chemical structures of the active compounds should be carefully verified.

Of these inhibitors, compound **6** displays a potent activity in inhibition of cell viability and cell growth in the HL-60 cell line. We further demonstrated that **6** induces apoptosis in cancer cells with high Bcl-2 expression but has no or very little effect in cancer cells with low Bcl-2 expression. Furthermore, using NMR methods, we conclusively demonstrated that **6** binds to the BH3 binding site in Bcl-X_L. Taken together, **6** represents a novel class of cell-permeable small-molecule inhibitors of Bcl-2 and a lead compound for further design and chemical modifications.

A number of factors may contribute to the successful discovery of these Bcl-2 small-molecule inhibitors. First, the high degree of homology between Bcl-2 and Bcl-X_L allows for an accurate modeling of the 3D structure of Bcl-2, in particular its binding site, which provides a solid structural basis for the identification of potential small-molecule inhibitors binding to this site. Second, the current version of the DOCK program employed in our structure-based computer screening takes the conformational flexibility of the small molecules into account. Inclusion of the conformational flexibility of the small molecules in structure-based computer screening is important because it is rare that a single conformation of a small molecule stored in the 3D database is the desired conformation for binding to the target molecule (Bcl-2). Third, the NCI open database provides a large number of unique synthetic compounds and natural products, which is an excellent database for drug lead discovery. Certain improvements can be made to our database searching strategy. For example, we used a single conformation of Bcl-2 in our database search. However, our lengthy MD simulation showed that Bcl-2 exhibits certain conformational flexibility in its binding site (data not shown) and some of the conformations are significantly different from the conformation used in our database search. Exploring the conformational flexibility of the Bcl-2 binding site could lead to the discovery of additional novel inhibitors of Bcl-2. Furthermore, we used a simple interaction energy function as implemented in the DOCK program to rank the potential Bcl-2 inhibitors identified in the computer screening. Thus, using a scoring function that has a better correlation with the binding affinity (binding free energy) may improve the yield of the active compounds and could lead to the discovery of additional and/or more potent novel Bcl-2 inhibitors.

The discovery of these novel, nonpeptide, cell-permeable, small-molecule Bcl-2 inhibitors represents the first but very exciting step toward the development of a novel cancer therapy that targets Bcl-2 for the treatment of breast, prostate, and many other forms of cancers with Bcl-2 protein overexpression. A small-molecule drug that inhibits the anti-apoptotic function of Bcl-2 is predicted to be particularly effective when used in combination with other conventional chemotherapeutic drugs or radiation therapy. Moreover, a potent cell-permeable small-molecule inhibitor also provides an invaluable research tool to further elucidate the function of Bcl-2 in vitro *and* in vivo. Extensive efforts to further optimize the small-molecule inhibitors of Bcl-2 discovered in this study through structure-based design are currently under way in our laboratories, and the results will be reported in due course.

Experimental Section

Homology Modeling. The sequence of human Bcl-2 was obtained from Gene Bank (entry gi4557355). The NMR structure of Bcl-X_L (PDB code 1BXL from the Protein Databank), which has 45% amino acid sequence identity, 56% sequence similarity, and 3% gaps with Bcl-2, was used as the template.[21] The structure of Bcl-2 was built using the homology-modeling program MODELLER (version 4.0).[26] MODELLER is most frequently used for comparative modeling of protein three-dimensional structure. More generally, MODELLER models protein 3D structure by satisfaction of spatial restraints.[24−26] The restraints used in our comparative modeling of Bcl-2 structure were automatically derived from the experimental 3D structure of Bcl-X_L by the MODELLER program. The output of MODELLER is the 3D structure models of Bcl-2 that satisfy these restraints as well as possible. The optimization is carried out by the variable target function procedure employing methods of conjugate gradients and molecular dynamics with simulated annealing.[26]

Further refinement was done using the molecular dynamics program CHARMM (version 27b2).[27] Hydrogen atoms were assigned to the modeled structure using the program QUANTA.[36] The Bak BH3 peptide was placed in the Bcl-2 BH3 domain binding site in the same orientation as in the NMR structure of Bcl-X_L in complex with the Bak BH3 peptide (1BXL in the Protein Databank).[21] The complex structure was solvated by inserting it into a 60 Å diameter TIP3P water sphere and deleting solvent molecules that have heavy atoms at less than 2.5 Å from any protein heavy atom. The MD simulation was done using the all-atom parameter set from the CHARMm force field as implemented in QUANTA,[36] a constant dielectric, $\epsilon = 1$, and constant temperature, $T = 300$ K. The leapfrog method with a 1 fs time step was applied for numerical integration. Long-range electrostatic forces were treated with the force switch method with a switching range of 8−12 Å. van der Waals forces were calculated with the shift method and a cutoff of 12 Å. The nonbond list was kept to 14 Å and updated heuristically. Solvent waters were kept from evaporating by using a spherical miscellaneous mean field potential as implemented in CHARMM.[27] The solvated protein was energy minimized using 100 cycles using the steepest descent method and an additional 1000 cycles using the adopted-basis Newton Raphson method. This was followed by a 3.0 ns MD simulation. The simulation was performed on an Origin2000 computer at the Advanced Biomedical Computing Center at the National Institutes of Health.

Structure-Based 3D Database Search. The refined structure of Bcl-2 from the Bak/Bcl-2 complex, obtained after the 3 ns MD simulation, was used for structure-based database searching of the NCI 3D database.[31] The program DOCK (version 4.0.1) was employed.[34] All residues within 8 Å from the Bak peptide were included in the binding site used for screening. United atom KOLLMAN charges were assigned for the protein using the BIOPOLYMER menu in the Sybyl program.[37] Because of its general applicability, the Geisterger method as implemented in Sybyl was used to assign charges to the NCI compounds. We searched the National Cancer Institute's 3D database of 206 876 small molecules and natural products that can be accessed by the public.[31]

The interactions between the Bak BH3 peptide and Bcl-2 in the modeled complex structures define the crucial binding elements between them. Thus, the spheres used in the DOCK program were defined in part by the coordinates of the Bak BH3 peptide in the modeled complex structure with Bcl-2. The conformational flexibility of the compounds from the database was considered, and their positions and conformations were optimized using single anchor search and torsion minimization. Fifty configurations per ligand building cycle and 100 maximum anchor orientations were used in the anchor-first docking algorithm. All docked configurations were energy minimized using 10 iterations and 2 minimization cycles. This combination of parameters resulted in an average of 26 CPU seconds per compound on a Silicon Graphics Indigo2 Impact with a 195 MHz R10,000 CPU. Several filters were used during database screening: compounds with more than 10 flexible bonds, with less than 10 heavy atoms, or with more than 50 heavy atoms were not considered. These essentially excluded highly flexible, very small or very large molecules. A scaling factor of 0.5 was used for the electrostatic interaction calculations. The sum of the electrostatic and van der Waals interactions as calculated in the DOCK program was used as the ranking score. The top-scoring 500 compounds were analyzed for structural diversity. All organometallic compounds were discarded. Chemical samples of 80 compounds were requested from the National Cancer Institute, and 35 had samples available for biological testing.

Chemical Samples of the NCI Open Compounds. The chemical samples of these 35 compounds were provided by the Drug Synthesis & Chemistry Branch, Developmental Therapeutics Program, Division of Cancer Treatment and Diagnosis, National Cancer Institute, National Institutes of Health. All compounds were dissolved at 10 mM in dimethyl sulfoxide (DMSO) prior to biological experiments.

Chemistry. General Procedure. All chemical reagents were commercially available. Melting points were determined on a MelTemp II apparatus, Laboratory Devices, and are uncorrected. Silica gel chromatography was performed on silica gel 60, 230−400 mesh (E. Merck). ^{1}H spectra were recorded on a Varian Mercury instrument at 300 MHz or on a Bruker AC-250 instrument at 250, and ^{13}C NMR spectra were recorded on a Bruker AC-250 instrument at 62.9 MHz. Spectra were referenced to the solvent in which they were run (7.24 ppm for ^{1}H ($CDCl_3$)). Elemental analyses were performed by Atlantic Microlab, Inc., Atlanta, GA. FAB mass spectra were performed on a VG-7070-EHF mass spectrometer, at unit resolution (isotopic mass), in the positive and/or negative ion mode. The sample matrix was 3-nitrobenzyl alcohol (NBA).

Structural Analysis of the NCI Compounds.

Compound **5**: FABMS 613.2 $(M + H)^+$; insoluble in either DMSO or chloroform.

Compound **6**: Identical mass and NMR spectra were obtained for this compound for the samples obtained from the NCI and synthesized in our laboratory. The data for this compound are provided in the Synthesis section below.

Compound **7**: ^{1}H NMR (DMSO-d_6, 300 MHz) δ 8.57 (d, 1H, J = 3.3 Hz), 8.55 (d, 1H, J = 3.3 Hz), 8.39−8.43 (m, 2H), 7.69 (t, 1H, J = 3.3 Hz), 7.67 (t, 1H, J = 3.3 Hz), 7.42−7.50 (m, 3 H); FABMS 305.4 $(M)^-$.

Compound **8**: ^{1}H NMR ($CDCl_3$, 300 MHz) δ 9.56 (d, 1H, J = 2.7 Hz), 8.57 (m, 1H), 8.22 (m, 1H), 7.91 (m, 1H), 7.71 (m, 2H), 7.52 (m, 1H), 7.32 (m, 1H); FABMS 222.1 $(M)^+$.

Compound **9**: FABMS 1241.8 $(M)^+$ or 352.3 $(M)^-$.

Compound **10**: FABMS 538 $(M)^-$.

Compound **11**: ^{1}H NMR (DMSO-d_6, 300 MHz) δ 10.92 (s, 1H), 9.48 (br s, 1H), 9.38 (s, 1H), 9.18 (br s, 1H), 8.0−8.2 (m, 4H), 7.90 (d, 1H, J = 7.2 Hz), 7.83 (d, 1H, J = 8.4 Hz), 7.35 (dd, 1H, J = 2.4, 7.2 Hz), 7.22 (t, 1H, J = 8.4 Hz), 7.05 (t, 1H, J = 7.2 Hz), 6.80 (d, 1H, J = 2.4 Hz), 6.61 (dd, 1H, J = 2.4, 8.4 Hz); FABMS 330.1 $(M + H)^+$.

Synthesis. 5,5′-Dimethoxy-2,2′-dinitrobibenzyl (41). To a solution of potassium *tert*-butoxide (16.11 g, 136.40 mmol) in ether (126.8 mL) and DMSO (6.34 mL) at −10 °C was added slowly 5-methyl-2-nitrotoluene (20 g, 119.65 mmol). The reaction mixture was stirred at −10 °C for 45 min, then allowed to warm to room temperature, and stirred for an additional 3 h. The reaction was quenched by adding water (50 mL) dropwise, and the mixture was extracted with CH_2Cl_2 (3 × 150 mL). The organic layers were gathered, dried with $MgSO_4$, filtered, and concentrated. The crude product was recrystallized in $CHCl_3$ to afford compound **41** (12.83 g, 38.57 mmol, 64%) as brown crystals: mp 193−195 °C; ^{1}H NMR (DMSO-d_6) δ 8.08 (d, 2H, J = 9.03 Hz), 7.07 (dd, 2H, J = 2.69, 9.03 Hz), 6.96 (d, 2H, J = 2.69 Hz), 3.88 (s, 4H), 3.40 (s, 6H); ^{13}C NMR (DMSO-d_6, 62.9 MHz) δ 162.65, 141.62, 138.52, 127.46, 116.80, 112.79, 55.97, 33.47. Anal. Calcd for $C_{16}H_{16}N_2O_6$: C, 57.83; H, 4.85; N 8.43. Found: C, 57,70; H 4.90; N 8.37.

5,5′-Dimethoxy-2,2′-diaminobibenzyl (42). A solution of 5,5′-dimethoxy-2,2′-dinitrobibenzyl (**41**) (12.0 g, 36.11 mmol) in ethanol (271 mL) was treated with 10% Pd/C (1.2 g), and hydrazine hydrate (7.37 mL, 236.52 mmol) was added dropwise over 10 min. The reaction mixture was stirred at rt for 30 min and then refluxed for 2 h. The hot solution was filtered through a short pad of Celite, and the catalyst was washed with hot benzene (500 mL) and hot 95% ethanol (250 mL). The filtrates were concentrated under reduced vacuum to give the crude product, which was recrystallized in benzene to afford **42** (9.64 g, 35.39 mmol, 98%) as dark green needles: mp 69−71 °C; ^{1}H NMR (DMSO-d_6, 250 MHz) δ 6.87−6.55 (m, 6H), 4.47 (br s, 4 H), 3.66 (s, 6H), 2.65 (s, 4H); ^{13}C NMR (DMSO-d_6, 62.9 MHz) δ 150.95, 139.62, 126.87, 115.58, 114.96, 111.73, 55.19, 30.13. Anal. Calcd for $C_{16}H_{20}N_2O_2$: C, 70.56; H, 7.40; N, 10.29. Found: C, 70.19; H, 7.45; N, 10.21.

2,9-Dimethoxy-11,12-dihydrodibenzo[*c*,*g*][1,2]-diazocine 5,6-Dioxide (6a) and 5,5′-Dimethoxy-2,2′-dinitrosobibenzyl (6b). A solution of **42** (2.46 g, 9.04 mmol) and sodium tungstate dihydrate (0.42 g, 1.26 mmol) in 95% ethanol (27.13 mL) and water (9.04 mL) was cooled to 5 °C and treated dropwise with 30% H_2O_2 (4.61 mL). The reaction mixture was stirred for 5 h at 5 °C, then 10 mL of a saturated aqueous solution of NH_4Cl was added, and the mixture was extracted with CH_2Cl_2 (3 × 30 mL). The organic phase was dried over Na_2SO_4, filtered, and concentrated under reduced pressure to afford the crude product. Recrystallization in CH_2Cl_2/hexanes afforded 1.22 g (4.06 mmol, 45%) of green crystals. The mother solution was concentrated under reduced pressure, and the residue purified by flash chromatography on silica gel with hexanes/ethyl acetate (3:1) as eluant to give an additional 0.431 g (1.47 mmol, 16%) of compounds **6a** and **6b** as green crystals, mp 136−138 °C.

Data for compound **6a** (ring cyclized isomer): ^{1}H NMR (DMSO-d_6, 250 MHz) δ 7.42 (d, 2H, J = 8.55 Hz), 6.89−6.83 (m, 4H), 3.76 (s, 6H), 3.07 (distorted d, 4H); ^{1}H NMR ($CDCl_3$, 250 MHz) δ 7.37 (d, 2 H, J = 8.79 Hz), 6.80 (dd, 2H, J = 2.69, 8.79 Hz), 6.66 (d, 2H, J = 2.69 Hz), 3.84 (s, 6H), 3.38 and 3.01 (A_2B_2, 4H).

Data for compound **6b** (open isomer): ^{1}H NMR (DMSO-d_6, 250 MHz) δ 7.19 (d, 2H, J = 2.69 Hz), 6.84−6.79 (m, 4H), 6.34 (d, 2H, J = 9.03 Hz), 4.36 (s, 4H), 3.91 (s, 6H); ^{1}H NMR ($CDCl_3$, 250 MHz) δ 6.97 (d, 2H, J = 2.44 Hz), 6.73 (dd, 2H, J = 2.44, 9.03 Hz), 6.54 (d, 2H, J = 9.03 Hz), 4.42 (s, 4H), 3.94 (s, 6H). Anal. Calcd for $C_{16}H_{16}N_2O_4$: C, 63.99; H 5.37, N 9.33. Found: C, 63.72; H 5.48, N 9.28. FABMS 300.9 $(M + H)^+$.

Bcl-2 FP Binding Assay. The fluorescence-labeled 16-mer peptide tracer Flu-Bak-BH3 (sequence GQVGRQLAIIGDDINR derived from the Bak BH3 domain) was synthesized and labeled at the amino terminus. The 46 kDa recombinant soluble GST-fused Bcl-2 protein was purchased from Santa Cruz Biotechnology (Santa Cruz, CA). The reaction was carried out in a total volume of 20 μL per well containing 10 μL of 1X phosphate-buffered saline, 5 μL of the GST-Bcl-2 protein, and 5 μL of peptide tracer. The reaction was incubated at room temperature for 20 min. The reading was taken at λ_{ex} = 485 nm and λ_{em} = 535 nm using the Ultra Reader (Tecan U.S. Inc., Research Triangle Park, NC). A series of validation experiments were performed by analyzing the maximal and minimal signals obtained by the background, buffer, Bcl-2 protein, tracer, and mixture of Bcl-2 protein and tracer. The K_d of binding between Bcl-2 protein and the 16-mer fluorescence-labeled peptide was determined by titration of Bcl-2 protein at a concentration range of 5.4−540 nM and fluorescent tracer concentration range of 0.145−1450 nM. The optimal binding was obtained at a final concentration of 290 nM fluorescent tracer and 270 nM Bcl-2 protein. To verify the specificity, binding of the labeled peptide was compared with that of the nonlabeled 16-mer peptide. The data indicate that nonlabeled 16-mer peptide was able to abrogate binding of the labeled tracer, with an IC_{50} of approximately 0.3 μM, a value similar to the value reported in the literature.

Initial screening of all compounds was carried out at 100 μM. A 5 μL sample of the test compound was added in reaction buffer to each of the wells containing tracer and Bcl-2 protein at the same concentration determined before. The final concentration of DMSO in all compounds was less than 1%. The final reading was taken after a 10 min incubation at room temperature. For IC_{50} determination of active compounds, six to seven point serial dilutions were made in triplicate starting at 100 μM.

Cells and Reagents. Human breast cell lines (T47D, MDA-231, MDA-453) and human Leukemia cells HL-60 were obtained from the American Type Culture Collection (ATCC). All tumor cell lines were grown and maintained in RPMI 1640 medium containing 10% FBS, except MDA-MB-231, which used Dulbecco's modified Eagle's medium as the basal medium.

Cultures were maintained in a humidified incubator at 37 °C and 5% CO_2.

Cell Viability and Growth Assays. Cell viability was determined by the trypan blue assay. Trypan blue is a polar dye that cannot cross intact cell membranes but crosses the membranes of necrotic cells and apoptotic cells undergoing secondary necrosis. Thus, it is a useful, rapid, and simple screening assay for viable cells. In this assay, cells (5000 cells/well) were plated in triplicate in 24-well plates with culture medium and various amounts of FBS. Various concentrations of drugs were added to the cells. Trypan blue dye was added 24 h later, and the percentage of viable cells was determined.

Cell growth was determined by the MTT assay. The MTT assay is a colorimetric assay that measures the reduction of MTT by mitochondrial succinate dehydrogenase. The MTT enters the cells and passes into the mitochondria, where it is reduced to an insoluble, colored, formazen product. The cells are then solubilized with an organic solvent (2-propanol), and the released, solubilized formazen reagent is measured spectrophotometrically. Since reduction of MTT can only occur in metabolically active cells, the level of activity is a measure of the viability of the cells. Cells (2000−4000 cells/well) were grown in medium with FBS, and various concentrations of drugs were added to the cells at the beginning. Four days later, MTT was added to each well and incubated for 4 h at 37 °C. Absorbency was measured with a Dynatech model MR700.

Assay of Apoptosis. For flow cytometry apoptosis assay, cell pellets were resuspended in 1× binding buffer (10 mM HEPES (pH 7.4), 0.15 M NaCl, 5 mM KCl, 1 mM $MgCl_2$, 1.8 mM $CaCl_2$) containing 1:100 dilution of Annexin V-FITC (Trevigen) and 50 μg/mL of propidium iodide and incubated at 4 °C for 15 min. The fluorescence of Annexin V-FITC and propidium iodide of individual cells was analyzed by FACscan.

NMR Experiments. a. Expression and Purification of the Bcl-X_L Protein. The recombinant Bcl-X_L protein was overexpressed from *Escherichia coli* BL21(DE3) and pET15b (Novagen, Darmstadt, Germany) expression vector with an N-terminal His tag. In this construct the putative C-terminal membrane-anchoring region (residues 214−237) and a loop between helix 1 and helix 2 (residues 49−88) were removed to facilitate the purification of the protein. This loop is previously shown to be dispensable for the anti-apoptotic activity of the protein.[19] The cells were grown in the minimum medium using $^{15}NH_4Cl$ as the sole nitrogen source to produce uniformly ^{15}N labeled protein.[39,40] The protein was purified with Ni-NTA resin (Novagen), and His tag was cleaved by thrombin digestion. The protein was further purified with NI-NTA resin and benzamidine Sepharose resin (Pharmacia, Piscataway, NJ).

b. NMR Data Acquisition and Analysis. The NMR experiments were performed on a Varian Inova 500 with pulse field gradient (PFG) HSQC with water flip back to maximize the signal intensity and to minimize the destruction from the water signal[41,42] (300 μM Bcl-X_L, 50 mM phosphate buffer (pH 7.3), 2 mM DTT at 25 °C). HSQC spectra of Bcl-X_L were recorded prior to (free Bcl-X_L) and after the addition of the concentrated **6** solution (the final concentration of **6** in the sample was 300 μM). Then two spectra were compared to identify the chemical shifts induced by the additions of the inhibitor. The NMR data were processed with the programs pipp and nmrDraw.[43,44]

Acknowledgment. The chemical samples used in our biological evaluations were provided by the Drug Synthesis & Chemistry Branch, Developmental Therapeutics Program, Division of Cancer Treatment and Diagnosis, National Cancer Institute, National Institutes of Health, and their help on this project is highly appreciated. We thank Professor Ziwei Huang from Thomas Jefferson University for providing us the Flu-Bak-BH3 peptide. We are grateful to Professor Gabriel Nunez from the University of Michigan Cancer Center for providing us the plasmid (pET30, Novagen) containing human Bcl-X_L gene and His tag. We thank Professor Frederick D. Greene II for sending us part of the thesis by David H. Bown, which described the synthetic methods for compound **6**. We are grateful to the Advanced Biomedical Computing Center at the NIH for providing us access to their Origin2000 supercomputer. Financial support from the CaPCure Foundation, the NCI SPORE Project (Grant P50CA058185), and the Lombardi Cancer Center is greatly appreciated.

References

(1) Gross, A.; McDonnell, J. M.; Korsmeyer, S. J. Bcl-2 family members and the mitochondria in apoptosis. *Genes Dev.* **1999**, *13*, 1899−1911.
(2) Adams, J. M.; Cory, S. The Bcl-2 protein family: arbiters of cell survival. *Science* **1998**, *281*, 1322−1326.
(3) Hawkins, C. J.; Vaux, D. L. The role of the Bcl-2 family of apoptosis regulatory proteins in the immune system. *Semin. Immunol.* **1997**, *9*, 25−33.
(4) Buolamwini, J. K. Novel anticancer drug discovery. *Curr. Opin. Chem. Biol.* **1999**, *3*, 500−509.
(5) Reed, J. C. Bcl-2 family proteins: strategies for overcoming chemoresistance in cancer. *Adv. Pharmocol.* **1997**, *41*, 501−553.
(6) Strasser, A.; Huang, D. C. S.; Vaux, D. L. The role of the bcl-2/ced-9 gene family in cancer and general implications of defects in cell death control for tumourigenesis and resistance to chemotherapy. *Biochim. Biophys. Acta* **1997**, *1333*, F151−F178.
(7) DiPaola, R. S.; Aisner, J. Overcoming bcl-2- and p53-mediated resistance in prostate cancer. *Semin. Oncol.* **1999**, *26*, 112−116.
(8) Ziegler, A.; Luedke, G. H.; Fabbro, D.; Altmann, K. H.; Stahel, R. A.; Zangemeister-Wittke, U. Induction of apoptosis in small-cell lung cancer cells by an antisense oligodexynucleotide targeting the BCl-2 coding sequence. *J. Natl. Cancer Inst.* **1997**, *89*, 1027−1036.
(9) Webb, A.; Cunningham, D.; Cotter, F.; Clarke, P. A.; Di Stefano, F.; Ross, P.; Corbo, M.; Dziewanowska, Z. BCl-2 antisense therapy in patients with nonhodgkin lymphoma. *Lancet* **1997**, *349*, 1137−1141.
(10) Jansen, B.; Schlagbauer-Wadl, H.; Brown, B. D.; Bryan, R. N.; Van Elsas, A.; Muller, M.; Wolff, K.; Eichler, H. G.; Pehamberger, H. BCl-2 antisense therapy chemosensitizes human melanoma in SCID mice. *Nat. Med.* **1998**, *4*, 232−234.
(11) Waters, J. S.; Webb, A.; Cunningham, D.; Clarke, P. A.; Raynaud, F.; Di Stefano, F.; Cotter, F. E. Phase I clinical and pharmacokinetic study of bcl-2 antisense oligonucleotide therapy in patients with non-hodgkin's lymphoma. *J. Clin. Onclol.* **2000**, *18*, 1812−1823.
(12) Piche, A.; Grim, J.; Rancourt, C.; Gomez-Navarro, J.; Reed, J. C.; Curiel, D. T. Modulation of Bcl-2 protein levels by an intracellular anti-Bcl-2 single-chain antibody increases drug-induced cytotoxicity in the breast cancer cell line MCF-7. *Cancer Res.* **1998**, *58*, 2134−2140.
(13) Chen, H. X.; Marshall, J. L.; Trocky, N.; Baidas, S.; Rizvi, N.; Ling, Y.; Bhagava, P.; Lippman, M. E.; Yang, D.; Hayes, D. F. A phase I study of bcl-2 antisense G3139 (Genta) and weekly docetaxel in patients with advanced breast cancer and other solid tumors. *Proc. Am. Soc. Clin. Oncol.*, in press.
(14) Wang, J.-L.; Zhang, Z.-J.; Choksi, S.; Shan, S.; Lu, Z.; Croce, C. M.; Alnemri, E. S.; Korngold, R.; Huang, Z. Cell permeable bcl-2 binding peptides: a chemical approach to apoptosis induction in tumor cells. *Cancer Res.* **2000**, *60*, 1498−1502.
(15) Wang, J.-L.; Liu, D.; Zhang, Z.-J.; Shan, S.; Han, X.; Srinivasula, S. M.; Croce, C. M.; Alnemri, E. S.; Huang, Z. Structure-based discovery of a novel organic compound that binds to Bcl-2 protein and induces apoptosis of tumor cells. *Proc. Natl. Acad. Sci. U.S.A.* **2000**, *97*, 7124−7129.
(16) Degterev, A.; Lugovskoy, A.; Cardone, M.; Mulley, B.; Wagner, G.; Mitchison, T.; Yuan, J. Identification of small-molecule inhibitors of interaction between the BH3 domain and Bcl-x_L. *Nat. Cell Biol.* **2001**, *3*, 173−182.
(17) Tzung, S.-P.; Kim, K. M.; Basanez, G.; Giedt, C. D.; Simon, J.; Zimmerberg, J.; Zhang, K. Y. J.; Hockenbery, D. M. Antimycin A mimics a cell-death-inducing Bcl-2 homology domain 3. *Nat. Cell Biol.* **2001**, *3*, 183−191.
(18) Petros, A. M.; Medek, A.; Nettesheim, D. G.; Kim, D. H.; Yoon, H. S.; Swift, K.; Matayoshi, E. D.; Oltersdorf, T.; Fesik, S. W. Solution structure of the antiapoptotic protein bcl-2. *Proc. Natl. Acad. Sci. U.S.A.* **2001**, *98*, 3012−3017.
(19) Muchmore, S. W.; Sattler, M.; Liang, H.; Meadows, R. P.; Harlan, J. E.; Yoon, H. S.; Nettesheim, D.; Chang, B. S.; Thompson, C. B.; Wong, S.-L.; Ng, S.-C.; Fesik, S. W. X-ray and NMR structure of human Bcl-X_L, an inhibitor of programmed cell death. *Nature* **1996**, *381*, 335−341.

(20) Aritomi, M.; Kunishima, N.; Inohara, N.; Ishibashi, Y.; Ohta, S.; Morikawa, K. Crystal structure of rat Bcl-X_L. Implications for the function of the Bcl-2 protein family. *J. Biol. Chem.* **1997**, *272*, 27886−27892.
(21) Michael, S.; Heng, L.; David, N.; Robert, P. M.; John, E. H.; Matthias, E.; Ho Sup, Y.; Suzanne, B. S.; Brian, S. C.; Andy, J. M.; Craig, B. T.; Stephen, W. F. Structure of Bcl-X_L-Bak peptide complex: recognition between regulators of apoptosis. *Science* **1997**, *275*, 983−986.
(22) Altschul, S. F.; Gish, W.; Miller, W.; Myers, E. W.; Lipman, D. J. Basic local alignment search tool. *J. Mol. Biol.* **1990**, *215*, 403−410.
(23) Altschul, S. F.; Madden, T. L.; Schäffer, A. A.; Zhang, J.; Zhang, Z.; Miller, W.; Lipman, D. J. Gapped BLAST and PSI-BLAST: a new generation of protein database search programs. *Nucleic Acids Res.* **1997**, *25*, 3389−3402.
(24) Sali, A.; Potterton, L.; Yuan, F.; van Vlijmen, H.; Karplus, M. Evaluation of comparative protein modeling by MODELLER. *Proteins: Struct., Funct., Genet.* **1995**, *23*, 318−326.
(25) Sali, A. Modeling mutations and homologous proteins. *Curr. Opin. Biotechnol.* **1995**, *6*, 437−451.
(26) See the MODELLER web site http://guitar.rockefeller.edu/modeller/modeller.html.
(27) Brooks, B. R.; Bruccoleri, R. E.; Olafson, B. D.; States, D. J.; Swaminathan, S.; Karplus, M. CHARMM: a program for macromolecular energy, minimization, and dynamics calculations. *J. Comput. Chem.* **1983**, *4*, 187−217.
(28) Cosulich, S. C.; Worrall, V.; Hedge, P. J.; Green, S.; Clarke, P. R. Regulation of apoptosis by BH3 domains in a cell-free system. *Curr. Biol.* **1997**, *7*, 913−920.
(29) Yin, X.-M.; Oltval, Z. N.; Korsmeyer, S. J. BH1 and BH2 domains of Bcl-2 are required for inhibition of apoptosis and heterodimerization with Bax. *Nature* **1994**, *369*, 321−323.
(30) Holinger, E. P.; Chittenden, T.; Lutz, R. J. Bak BH3 peptides antagonize Bcl-X_L function and induce apoptosis through cytochrome c-independent activation of caspases. *J. Biol. Chem.* **1999**, *274*, 13298−13304.
(31) Milne, G. W. A.; Nicklaus, M. C.; Wang, S.; Driscoll, J.; Zaharevitz, D. The NCI drug information system 3D database, *J. Chem Inf. Comput. Sci.* **1994**, *34*, 1219−1224.
(32) Voigt, J. H.; Bienfait, B.; Wang, S.; Nicklaus, M. C. Comparison of the NCI Open Database with Seven Large Chemical Structural Databases, *J. Chem. Inf. Comput. Sci.* **2001**, *41*, 702−712
(33) Kuntz, I. D.; Blaney, J. M.; Oatley, S. J.; Langridge, R.; Ferrin, T. E. A geometric approach to macromolecule-ligand interactions. *J. Mol. Biol.* **1982**, *161*, 269−288.
(34) Ewing, T. J. A.; Kuntz, I. D. Critical evaluation of search algorithms for automated molecular docking and database screening. *J. Comput. Chem.* **1997**, *18*, 1175−1189.
(35) Bown, D. H. Synthesis and investigation of aryl azo dioxide-bisnitroso systems. Ph.D. Thesis (thesis supervisor Professor Frederick D. Greene II), Department of Chemistry, Massachusetts Institute of Technology, Cambridge, MA, 1983.
(36) QUANTA, a molecular modeling system, is supplied by Molecular Simulations Inc., San Diego, CA.
(37) Sybyl, a molecular modeling system, is supplied by Tripos, Inc., St. Louis, MO 63144.
(38) Koradi, R.; Billeter, M.; Wuthrich, K. MOLMOL: a program for display and analysis of macromolecular structures. *J. Mol. Graphics* **1996**, *14*, 51−55.
(39) Cai, M. L.; Huang, Y.; Sakaguchi, K.; Clore, G. M.; Gronenborn, A. M.; Craigie, R. An efficient and cost-effective isotope labeling protocol for proteins expressed in *Escherichia coli*. *J. Biomol. NMR* **1998**, *11*, 97−102.
(40) Jansson, M.; Li, Y. C.; Jendeberg, L.; Anderson, S.; Montelione, G. T.; Nilsson, B. High-level production of uniformly N-15- and C-13-enriched fusion proteins in *Escherichia coli*. *J. Biomol. NMR* **1996**, *7*, 131−141.
(41) Grzesiek, S.; Bax, A. The Importance of Not Saturating H_2O in Protein NMR−Application to Sensitivity Enhancement and Noe Measurements. *J. Am. Chem. Soc.* **1993**, *115*, 12593−12594.
(42) Sheppard, G. S.; Davidsen, S. K.; Fesik, S. W.; Steinman, D. H.; Carrera, G. M.; Florjancic, A. S.; Hajduk, P. J.; Shuker, S. B.; Olejniczak, E. T.; Nettesheim, D.; Meadows, R. P.; Nagy, I.; Marcotte, P.; Magoc, T. J.; Morgan, D. W.; Summers, J. B. SAR by NMR as a novel tool for lead generation: Discovery of a potent series of non-peptide inhibitors of stromelysin (MMP-3). *Abstr. Pap.−Am. Chem. Soc.* **1997**, *213*, 81.
(43) Delaglio, F.; Grzesiek, S.; Vuister, G. W.; Zhu, G.; Pfeifer, J.; Bax, A. NMRPipe: a multidimensional spectral processing system based on UNIX pipes. *J. Biomol. NMR* **1995**, *6*, 277−293.
(44) Garrett, D. S.; Powers, R.; Gronenborn, A. M.; Clore, G. M. A common sense approach to peak picking in two-, three-, and four-dimensional double and triple-resonance heteronuclear magnetic resonance spectroscopy. *J. Magn. Reson., Ser. B* **1991**, *95*, 214−220.

JM010016F